Séminaire Lotharingien de Combinatoire **89B** (2023)
Article #47, 12 pp.

Proceedings of the 35th Conference on Formal Power Series and Algebraic Combinatorics (Davis)

The BCFW Tiling of the Amplituhedron

Chaim Even-Zohar*[1], Tsviqa Lakrec†[2], Ran J. Tessler‡[3]

[1] *Faculty of Mathematics, Technion*
[2] *Institute of Mathematics, University of Zürich*
[3] *Department of Mathematics, Weizmann Institute of Science*

Abstract. The amplituhedron $\mathcal{A}_{n,k,4}$ is a geometric object, discovered by Arkani-Hamed and Trnka (2013) in the study of scattering amplitudes in quantum field theories. They conjecture that $\mathcal{A}_{n,k,4}$ admits a decomposition into tiles, which is based on a certain combinatorial structure. The tiles are images of BCFW positroid cells in the nonnegative Grassmannian $\mathrm{Gr}_{k,n}^{\geq}$ that arise from the Britto–Cachazo–Feng–Witten recurrence (2005).

In a recent preprint we prove this conjecture. The full paper is available online at `https://arxiv.org/pdf/2112.02703`. In this extended abstract we review the amplituhedron and its BCFW tiling, and outline the main ideas from the proof.

1 The Amplituhedron

The amplituhedron $\mathcal{A}_{n,k,m}$ is the image of a positive map $\mathrm{Gr}_{k,n}^{\geq} \xrightarrow{\tilde{Z}} \mathrm{Gr}_{k,(k+m)}$ which "projects" the nonnegative real Grassmannian to a smaller Grassmannian. Here we target the fundamental problem of triangulating the amplituhedron into images of positroid cells of $\mathrm{Gr}_{k,n}^{\geq}$. We first briefly review the definitions of all these objects.

The real *Grassmannian* $\mathrm{Gr}_{k,n}$ is the variety of k-dimensional linear subspaces in $\mathbb{R}^n$. It is concretely represented as the quotient space $\mathrm{Gr}_{k,n} = \mathrm{GL}_k(\mathbb{R}) \setminus \mathrm{Mat}^*_{k\times n}(\mathbb{R})$. This means full-rank $k \times n$ real matrices modulo row operations performed by invertible $k \times k$ matrices. For a representative $k \times n$ matrix C, every set $I \subseteq \{1, \ldots, n\}$ of k columns defines a *Plücker coordinate* $P_I(C)$ as the determinant of the $k \times k$ minor corresponding to I. Using all Plücker coordinates, the Grassmannian embeds in the $\left(\binom{n}{k} - 1\right)$-dimensional real projective space. The *positive Grassmannian* $\mathrm{Gr}_{k,n}^{>}$ is the subset of points in the Grassmannian with all $P_I > 0$. Its closure is the *nonnegative Grassmannian* $\mathrm{Gr}_{k,n}^{\geq}$, with all $P_I \geq 0$.

*chaime@technion.ac.il. C.E. thanks the Lloyds Register Foundation's Alan Turing Institute programme on Data-Centric Engineering for their support during part of the research.

†tsviqa@gmail.com T.L. was supported by ERC 2020 grant HomDyn, grant no. 833423 and by SNSF grant Dynamical Systems, grant no. 188535.

‡ran.tessler@weizmann.ac.il. R.T., incumbent of the Lillian and George Lyttle Career Development Chair, was supported by the ISF grant no. 335/19 and by a research grant from the Center for New Scientists of Weizmann Institute.

The theory of positivity for algebraic groups and partial flag varieties, and in particular the positive Grassmannian, was developed by Lusztig [34]. It was further studied by Rietsch [42, 41, 40], Marsh and Rietsch [35], Fomin and Zelevinsky [18, 19, 20], and Postnikov [38, 39]. Postnikov developed a rich combinatorial picture of the nonnegative Grassmannian and its cell decomposition into positroid cells. An open *positroid cell* $S \subseteq \mathrm{Gr}^{\geq}_{k,n}$ comprises the points where a certain subset of the Plücker coordinates are positive, i.e., all C such that $P_I(C) > 0$ for $I \in M$ and $P_I(C) = 0$ for $I \notin M$, for some set M. These positroid cells admit explicit parametrizations by $(0,\infty)^d$ for some $d = \dim S$. They correspond to various combinatorial objects such as graphs, tableaux, and permutations, which play a role in this work. The positive Grassmannian bears relations and applications to diverse areas, including cluster algebras, tropical geometry, and integrable systems [43, 27, 28, 33, 44]. A recent application to scattering amplitudes in theoretical physics by Arkani-Hamed et. al. [5] motivates the definition of the amplituhedron by Arkani-Hamed and Trnka [11], which is the focus of this work.

The amplituhedron depends on an additional parameter $m \leq n-k$ and a real matrix $Z \in \mathrm{Mat}^{>}_{n\times(k+m)}$. This notation means that Z is assumed to be a *positive* matrix, in the sense that each one of its $\binom{n}{k+m}$ maximal minors has a positive determinant. The right multiplication by Z induces a well-defined map $\widetilde{Z} : \mathrm{Gr}^{\geq}_{k,n} \to \mathrm{Gr}_{k,(k+m)}$ In terms of representative matrices, the image of a point $C \in \mathrm{Gr}^{\geq}_{k,n}$ is $CZ \in \mathrm{Gr}_{k,k+m}$, and the image of a cell $S \subseteq \mathrm{Gr}^{\geq}_{k,n}$ is $\widetilde{Z}(S) = \{CZ : C \in S\}$. The tree *amplituhedron* is defined as the image of the entire nonnegative Grassmannian:

$$\mathcal{A}_{n,k,m}(Z) \;=\; \left\{ CZ \,:\, C \in \mathrm{Gr}^{\geq}_{k,n} \right\} \;\subset\; \mathrm{Gr}_{k,(k+m)}.$$

The amplituhedron is known to be a proper subspace of full dimension km. Since many of its structural properties do not seem to depend on the choice of Z, we often denote the amplituhedron by $\mathcal{A}_{n,k,m}$ and argue for any fixed Z. See [11, 5, 24, 13] for an exposition of the topic and physical background. The amplituhedron has been much studied in recent years [12, 25, 32, 23, 26, 31, 36, 37]. Generalizations to non-tree level or other physical theories have been considered [6, 3, 9, 8, 46, 7]. Its mathematical foundations are being studied under the name *positive geometries* [4, 30].

2 Tiling

The structure of the amplituhedron is less understood than that of the nonnegative Grassmannian. It is desirable to establish ways to subdivide $\mathcal{A}_{n,k,m}$ into simple pieces, in analogy to triangulations of a polytope for example. The following definition suggests that this can be achieved using homeomorphic images under Z of positroid cells of the appropriate dimension.

Definition 1 (Bao and He [12]). A *triangulation* of the amplituhedron $\mathcal{A}_{n,k,m}$ is a collection $\mathcal{T}$, of km-dimensional open positroid cells of the nonnegative Grassmannian $\mathrm{Gr}_{k,n}^{\geq}$, that satisfies the following properties for every $Z \in \mathrm{Mat}_{n\times(k+m)}^{>}$:

- *Injectivity*: $S \to \widetilde{Z}(S)$ is an injective map for every cell $S \in \mathcal{T}$.
- *Separation*: $\widetilde{Z}(S)$ and $\widetilde{Z}(S')$ are disjoint for every two cells $S \neq S'$ in $\mathcal{T}$.
- *Surjectivity*: $\bigcup_{S\in\mathcal{T}} \widetilde{Z}(S)$ is an open dense subset of $\mathcal{A}_{n,k,m}(Z)$.

The case $m = 4$ is the most relevant to physics, being applicable to scattering amplitudes in planar $\mathcal{N}$=4 supersymmetric Yang–Mills theory (SYM). Recurrence relations for computing scattering amplitudes arise from the work of Britto, Cachazo, Feng, and Witten [14, 15]. The BCFW recurrence translates into a recursive definition of a collection of $4k$-dimensional positroid cells in the nonnegative Grassmannian $\mathrm{Gr}_{k,n}^{\geq}$. These cells correspond to different terms that add up to the scattering amplitude, see [11, 5]. A direct definition, based on a canonical way of applying BCFW, was given by Karp, Williams, and Zhang [26]. This collection is named the *BCFW cells* and denoted here by $\mathcal{BCFW}_{n,k}$ – see definitions in Section 3 below. It contains $\frac{1}{k+1}\binom{n-3}{k}\binom{n-4}{k}$ cells. The relation between scattering amplitudes and the amplituhedron is based on the following conjecture.

Conjecture 2 (Arkani-Hamed and Trnka [11]). *For every $k \geq 1$ and $n \geq k+4$, the cells $\mathcal{BCFW}_{n,k}$ form a triangulation of the amplituhedron $\mathcal{A}_{n,k,4}$.*

In our full preprint [16] we prove this conjecture. We develop new machinery for analyzing how positroid cells map into the amplituhedron. We devise a scheme of procedures for recursively constructing subsets of the positive Grassmannian, including all BCFW cells. We derive distinctive characteristics of their images, such as functions having constant sign on a given cell, and keep track of their evolution as the construction proceeds. These techniques let us locate preimages in order to show injectivity, compare two cells to tell their images apart, and analyze boundaries between cells. We demonstrate our approach in the case of Conjecture 2, showing that the BCFW cells triangulate the $m = 4$ amplituhedron in the sense of Definition 1. Namely, we prove the following three properties for every $k \geq 1$, $n \geq k+4$ and positive $Z \in \mathrm{Mat}_{n\times(k+4)}^{>}$.

Theorem 3. *The map $S \to \widetilde{Z}(S)$ is injective for every cell $S \in \mathcal{BCFW}_{n,k}$.*

Theorem 4. *The images $\widetilde{Z}(S)$, $\widetilde{Z}(S')$ are disjoint for each two different cells $S, S' \in \mathcal{BCFW}_{n,k}$.*

Theorem 5. *The union of $\widetilde{Z}(S)$ over $S \in \mathcal{BCFW}_{n,k}$ is an open dense subset of $\mathcal{A}_{n,k,4}(Z)$.*

Another outcome of our analysis is a characterization of the boundary of the $m = 4$ amplituhedron. We also show that this is a *good* triangulation, in the sense that every internal wall is an image of a boundary stratum between two BCFW cells. For every positive Z, we deduce that the interior of the amplituhedron $\mathcal{A}_{n,k,4}(Z)$ is homeomorphic to an open ball. We note that Galashin, Karp and Lam [22] proved that $\mathcal{A}_{n,k,m}(Z)$

is homeomorphic to a closed ball for some specific choice of a positive matrix Z, for every even m. See the full preprint [16, Corollaries 8.7-8.8 and Theorem 9.2] for the precise formulation of our results, which may be steps towards establishing a regular CW decomposition [21] for $\mathcal{A}_{n,k,4}(Z)$.

Many of the techniques we develop generalize to other values of m and other triangulations and families of positroid cells. These tools are useful for manipulating functions of the amplituhedron's coordinates, showing injectivity of the amplituhedron map, separating between cells, and boundary cancellations. We establish a high-level decomposition of the amplituhedron [16, Theorem 9.6], and in a future paper we obtain as a corollary more general triangulations from the different ways to apply the BCFW recursion.

Related Work: Since Conjecture 2 was posed, triangulations of $\mathcal{A}_{n,k,m}$ have been studied for various values of m and k. Karp and Williams give a triangulation of $\mathcal{A}_{n,k,1}$ [25]. The case of $\mathcal{A}_{n,1,m}$ is a cyclic polytope in projective space [45]. Galashin and Lam introduce the parity duality, which relates triangulations of $\mathcal{A}_{n,k,m}$ with triangulations of $\mathcal{A}_{n,n-m-k,m}$ [23]. Karp, Williams and Zhang prove injectivity and separation in the special case $\mathcal{A}_{n,2,4}$ using domino forms and an exhaustive case analysis [26]. Bao and He prove a triangulation of $\mathcal{A}_{n,k,2}$ based on BCFW-like cells [12]. Parisi, Sherman-Bennett and Williams use twistor coordinates to establish many triangulations of $\mathcal{A}_{n,k,2}$, and relate them to triangulations of the hypersimplex [37]. For other related results, see recent surveys by Williams [48] and Lam [30].

Our methods are inspired by several ideas from previous works on Conjecture 2. We use matrix operations similar to Lam [29] and Bao and He [12] in order to manipulate cells. Our basic ingredient in separating cells is the twistor coordinates, similarly to Parisi, Sherman-Bennett and Williams [37]. Our analysis of boundaries is reminiscent with that of Agarwala and Marcott [1]. We use the domino form by Karp, Williams, Zhang, and Thomas [26] to represent BCFW cells. In particular, we settle their Conjecture A.7 – see Theorem 8 in the next section.

3 BCFW Tiles

In the seminal work of Postnikov [38], several families of combinatorial structures are employed to define and study the cells of the nonnegative Grassmannian. A few objects that are identified with positroid cells are: certain bicolored planar networks, known as *plabic graphs*; certain 0/1-filled Young tableaux, known as $\oplus$-*diagrams* [47]; and permutations with two kinds of fixed points, known as *decorated permutations*.

More combinatorial representations are available for the special class of BCFW cells. These are given by a particular family of plabic graphs in [5, with a certain rotation by two], and by pairs of *noncrossing lattice walks* in [26], describing additional equivalent viewpoints using *binary trees*, *Dyck paths* and *domino matrices*. For our purposes in this extended abstract, it is convenient to define the BCFW cells by chord diagrams – yet another combinatorial representation, which is a variant of the *Wilson loop diagrams* used by Agarwala, Marin-Amat and Marcott [2, 1].

Definition 6. A *chord diagram* is a straight horizontal line in the plane, which contains n *markers* labeled $\{1, 2, \ldots, n\}$ left-to-right, and k *chords* $c_1, c_2, \ldots, c_k$ above that line, whose *tail* and *head* lie left-to-right on the line, such that:

(a) No chord starts or ends on a marker.
(b) No two chords intersect.
(c) No chord starts before the marker 1 or ends after $n-1$.
(d) No two chords *start* on the same segment between two markers.
(e) No chord starts and ends on the same segment, nor on adjacent segments.

See Figure 1 for an example of a chord diagram. The number of chord diagrams with n markers and k chords is the Narayana number $\frac{1}{k+1}\binom{n-3}{k}\binom{n-4}{k}$.

For every chord c_l we denote by (i_l, i_l+1) the segment that contains its tail, and by (j_l, j_l+1) the one that contains its head. We call c_l a *top* chord if it is not nested in another chord. Otherwise c_l is a child of the chord c_m which is immediately above it.

Karp, Williams, Zhang and Thomas [26, Appendix A] suggest representing the points in the BCFW cells by special matrices, whose rows are called *domino bases*. Here we redefine these matrices via their one-to-one correspondence to chord diagrams.

Definition 7. The *domino matrix* that corresponds to a given chord diagram with n markers and k chords is a $k \times n$ real matrix depending on $5k$ real variables. Order the chords left-to-right by their tails, and fill row l using c_l as follows.

(a) Write the variables $(\alpha_l, \beta_l, \gamma_l, \delta_l)$ at the tail and head columns (i_l, i_l+1, j_l, j_l+1).
(b) If c_l is a top chord, write another variable ε_l at the last column n.
(c) If c_l is a child of c_m, add $(\varepsilon_l\alpha_m, \varepsilon_l\beta_m)$ at the columns (i_m, i_m+1) of the parent's tail.
(d) In the remaining columns, write zeros.

See Figure 1 for an example of a domino matrix. Note that every row is supported on five or six entries. This form is useful for analyzing the amplituhedron map.

In order to make sure that these domino matrices are nonnegative, we define the following set of *sign rules*. The tail variables α_l and β_l are always positive. The sign of the head variables γ_l and δ_l is $(-1)^{\mathrm{below}(c_l)}$, depending on the number of chords below c_l. The sign of ε_l is $(-1)^{k-l}$ if c_l is a top chord, and $(-1)^{l-m-1}$ if it is a child of another chord c_m. Moreover, if a chord c_m and its child c_l end in the same segment between markers then $\delta_l/\gamma_l < \delta_m/\gamma_m$, and if a chord c_l starts in the segment where c_m ends then $\delta_m/\gamma_m < \beta_l/\alpha_l$. Unless stated otherwise, when considering a domino matrix we assume that it satisfies these rules.

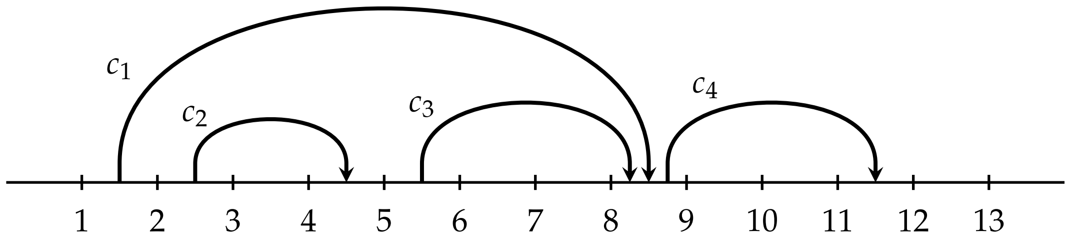

$$\begin{pmatrix} \alpha_1 & \beta_1 & 0 & 0 & 0 & 0 & 0 & \gamma_1 & \delta_1 & 0 & 0 & 0 & \varepsilon_1 \\ \varepsilon_2\alpha_1 & \varepsilon_2\beta_1+\alpha_2 & \beta_2 & \gamma_2 & \delta_2 & 0 & 0 & 0 & 0 & 0 & 0 & 0 & 0 \\ \varepsilon_3\alpha_1 & \varepsilon_3\beta_1 & 0 & 0 & \alpha_3 & \beta_3 & 0 & \gamma_3 & \delta_3 & 0 & 0 & 0 & 0 \\ 0 & 0 & 0 & 0 & 0 & 0 & 0 & \alpha_4 & \beta_4 & 0 & \gamma_4 & \delta_4 & \varepsilon_4 \end{pmatrix}$$

Figure 1: A chord diagram with $n = 13$ markers and $k = 4$ chords, and below it the corresponding domino matrix. The sign rules in this case give: $\alpha_i, \beta_i, \gamma_i, \delta_i > 0$ for all i; $\varepsilon_2, \varepsilon_4 > 0$ while $\varepsilon_1, \varepsilon_3 < 0$; and $\delta_3/\gamma_3 < \delta_1/\gamma_1 < \beta_4/\gamma_4$.

We prove in [16] the following theorem, asserting that under the sign rules a domino matrix provides a one-to-one parametrization of a $4k$-dimensional positroid cell in $\mathrm{Gr}_{k,n}^{\geq}$. Moreover, we show that the positroid cells that correspond to all chord diagrams via these matrices are exactly the BCFW cells.

Theorem 8. *Every point in a BCFW cell has a representative domino matrix, which corresponds to the chord diagram associated with that cell. This representation is unique up to rescaling each row by a positive number. Conversely, every domino matrix that satisfies the sign rules represents a point in the corresponding BCFW cell.*

See [16, Theorem 3.37, Proposition 7.3] for a more detailed formulation of this result. For the purposes of this overview, assume Theorem 8 to *define* the BCFW positroid cells, as those arising from all n-marker k-chord diagrams via Definitions 6-7. For an example, see $\mathcal{BCFW}_{7,2}$ in Figure 2. In [16, Sections 2-3] we show that this definition is equivalent to that of Karp, Williams, and Zhang [26, Section 5] who used plabic graphs based on Arkani-Hamed et al. [5, Section 16].

A key ingredient in the proof of Theorem 8 is a recursive algorithm that gradually constructs a domino matrix by a sequence of simple matrix operations that preserve positivity [16, Sections 3.1-3.2]. In short, these operations are: insertion of a zero column, insertion of a new row and a unit column, and adding a multiple of one column to an adjacent one, with a new positive variable as the coefficient. This explicit iterative construction allows us to apply induction on the structure of the chord diagram also in the subsequent proofs of Theorems 3, 4, and 5.

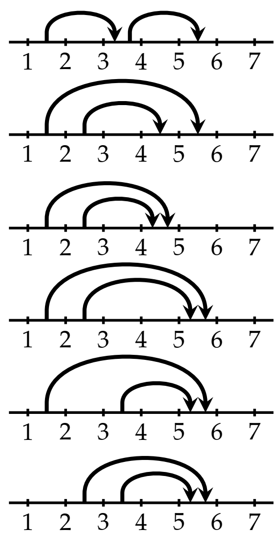

(A) $$\begin{pmatrix} \alpha_1 & \beta_1 & \gamma_1 & \delta_1 & 0 & 0 & \varepsilon_1 \\ 0 & 0 & \alpha_2 & \beta_2 & \gamma_2 & \delta_2 & \varepsilon_2 \end{pmatrix}$$

(B) $$\begin{pmatrix} \alpha_1 & \beta_1 & 0 & 0 & \gamma_1 & \delta_1 & \varepsilon_1 \\ \varepsilon_2\alpha_1 & \varepsilon_2\beta_1+\alpha_2 & \beta_2 & \gamma_2 & \delta_2 & 0 & 0 \end{pmatrix}$$

(C) $$\begin{pmatrix} \alpha_1 & \beta_1 & 0 & \gamma_1 & \delta_1 & 0 & \varepsilon_1 \\ \varepsilon_2\alpha_1 & \varepsilon_2\beta_1+\alpha_2 & \beta_2 & \gamma_2 & \delta_2 & 0 & 0 \end{pmatrix}$$

(D) $$\begin{pmatrix} \alpha_1 & \beta_1 & 0 & 0 & \gamma_1 & \delta_1 & \varepsilon_1 \\ \varepsilon_2\alpha_1 & \varepsilon_2\beta_1+\alpha_2 & \beta_2 & 0 & \gamma_2 & \delta_2 & 0 \end{pmatrix}$$

(E) $$\begin{pmatrix} \alpha_1 & \beta_1 & 0 & 0 & \gamma_1 & \delta_1 & \varepsilon_1 \\ \varepsilon_2\alpha_1 & \varepsilon_2\beta_1 & \alpha_2 & \beta_2 & \gamma_2 & \delta_2 & 0 \end{pmatrix}$$

(F) $$\begin{pmatrix} 0 & \alpha_1 & \beta_1 & 0 & \gamma_1 & \delta_1 & \varepsilon_1 \\ 0 & \varepsilon_2\alpha_1 & \varepsilon_2\beta_1+\alpha_2 & \beta_2 & \gamma_2 & \delta_2 & 0 \end{pmatrix}$$

Figure 2: The full triangulation of the amplituhedron $\mathcal{A}_{7,2,4}$ with 6 tiles given as chord diagrams and domino matrices. By the sign rules, all variables are positive, except for ε_1 in tiles (A)-(F) and γ_1, δ_1 in tiles (B)-(F) which are negative. Also, $\delta_1/\gamma_1 < \beta_2/\alpha_2$ in tile (A), and $\delta_2/\gamma_2 < \delta_1/\gamma_1$ in tiles (C)-(F), where two chords occur in one segment.

4 Proof Overview

Theorems 3, 4, and 5 assert that the amplituhedron $\mathcal{A}_{n,k,4}$ is triangulated by the images of the BCFW cells, as characterized above using chord diagrams, domino matrices and Theorem 8. We now sketch the main tools and ideas that appear in the proofs.

We work with the *twistor coordinates* for the amplituhedron, which are a set of real-valued functions that take into account the positive matrix Z. They were introduced by Arkani-Hamed and Trnka [11], and used by Arkani-Hamed, Thomas and Trnka [10] to develop a combinatorial and topological picture of the amplituhedron. Parisi, Sherman-Bennett and Williams [37] used them to characterize the Z-images of a large family of positroid cells giving rise to triangulations of $\mathcal{A}_{n,k,2}$.

Definition 9. Given two matrices $Y \in \mathrm{Mat}_{k\times(k+4)}$ and $Z \in \mathrm{Mat}_{n\times(k+4)}$, the twistor of $a, b, c, d \in \{1, \ldots, n\}$ is defined as the following $(k+4)\times(k+4)$ determinant:

$$\langle a\, b\, c\, d \rangle \;=\; \det\left[Y_1\, Y_2\, \cdots\, Y_k\, Z_a\, Z_b\, Z_c\, Z_d\right]$$

Here Y_i and Z_i denote rows in the matrices Y and Z. As usual, Z is the positive matrix that defines the amplituhedron map. The matrix Y represents a point in its image, which lies in $\mathrm{Gr}_{k,k+4}$. Note that the twistors are defined on the amplituhedron up to global rescaling. Since Z and $Y = CZ$ are usually fixed and understood from the context, they are omitted from the twistor notation.

In section 4 of [16] we devise general tools for analyzing the *promotion* of twistors, which is the way they transform when the above-mentioned matrix operations are applied to C, or when a chord is added to the diagram. This machinery is instrumental in the proofs of Theorems 3-5, which rely on the recursive construction of domino matrices using a sequence of matrix operations and their effects on twistors.

Injectivity

Theorem 3 asserts that the amplituhedron map $\widetilde{Z} : S \to \mathcal{A}_{n,k,4}$ is injective for each BCFW cell S. Our proof in [16, Section 5] goes by solving the inverse problem. Given a point in the image $\widetilde{Z}(S)$ we find its unique preimage in S. By Theorem 8 above, it is sufficient to construct a domino matrix C, given the image CZ. This is done based on the hierarchical structure of the corresponding chord diagram, where the nonzero entries of C are recovered in parent-to-child order.

Every top chord c_l corresponds to a domino matrix row C_l supported on five entries $(\alpha_l, \beta_l, \gamma_l, \delta_l, \varepsilon_l)$, say in the respective columns $a, b, c, d, e \in \{1, \ldots, n\}$. By linear algebra [16, Lemma 4.34], it follows that the two following vectors must be proportional:

$$(\alpha_l, \beta_l, \gamma_l, \delta_l, \varepsilon_l) \;\propto\; (+\langle b\,c\,d\,e\rangle,\; -\langle a\,c\,d\,e\rangle,\; +\langle a\,b\,d\,e\rangle,\; -\langle a\,b\,c\,e\rangle,\; +\langle a\,b\,c\,d\rangle)$$

Thus we can recover the matrix row C_l unless all five twistors vanish at some point. We rule out the latter possibility based on the domino representation as well.

Now suppose that a chord c_l is a child of another chord c_m whose entries have already been recovered. Then, the row C_l might have six nonzero entries: $(\varepsilon_l \alpha_m, \varepsilon_l \beta_m, \alpha_l, \beta_l, \gamma_l, \delta_l)$ in columns $a, b, c, d, e, f \in \{1, \ldots, n\}$. However, we already know the proportion between α_m and β_m from the parent's row. The contribution of the rows Z_a and Z_b is proportional to the combination $\alpha_m Z_a + \beta_m Z_b$. In the same way as before, we recover an "effective" preimage row of five entries, again verifying that they never vanish. This leads to expressions by twistors for all six entries, as demonstrated in the following example.

Example 10. Consider the BCFW cell (E) from Figure 2. A preimage of this domino form can be expressed using twistors as follows.

$$\begin{pmatrix} -\langle 2567\rangle & +\langle 1567\rangle & 0 & 0 & -\langle 1267\rangle & +\langle 1257\rangle & -\langle 1256\rangle \\ \alpha_1\langle 3456\rangle & \beta_1\langle 3456\rangle & -\langle X456\rangle & +\langle X356\rangle & -\langle X346\rangle & +\langle X345\rangle & 0 \end{pmatrix}$$

where $\alpha_1 = -\langle 2567\rangle$, $\beta_1 = \langle 1567\rangle$ and we write formally $X = \alpha_1 1 + \beta_1 2$ and expand linearly. For example, the entry $-\langle X346\rangle$ equals $\langle 2567\rangle\langle 1346\rangle - \langle 1567\rangle\langle 2346\rangle$.

As shown in the above example, our solution for the inverse problem expresses the preimage as a domino matrix, where each entry is a homogeneous polynomial in the twistor coordinates. We call such a polynomial in twistors a *functionary*.

Separation

Theorem 4 asserts that every two BCFW cells $S, S' \in \mathcal{BCFW}_{n,k}$ have disjoint images in the amplituhedron $\mathcal{A}_{n,k,4}$. We prove this by finding a *separating functionary*. This means a polynomial in the twistors that attains fixed and opposite signs on $\widetilde{Z}(S)$ and $\widetilde{Z}(S')$, for every positive matrix Z. The functionary is combinatorially constructed by induction on the chord diagrams of S and S'. The proof that it separates relies on our study of twistor promotions under matrix operations. To illustrate these promotions, they look similar to Example 10 where a twistor "transforms" into a quadratic functionary.

To give a taste of how the separation works, we sketch here the inductive definition of the separating functionary, and refer to the full preprint [16, Section 6] for more details and proofs, and to [17] for a `Sage` implementation. Compare the rightmost top chords of S and S'. Let $I = (a, b, c, d, n)$ and $I' = (a', b', c', d', n)$ be the respective supports of their domino rows. Then,

- If $d' < d$, take the following twistor as a separating functionary: $\langle a\, b\, c\, n\rangle$
- If $(c, d) = (c', d')$ but $b \neq b'$, take the quadratic: $\langle a\, b\, c\, n\rangle\langle a'\, b'\, d\, n\rangle - \langle a\, b\, d\, n\rangle\langle a'\, b'\, c\, n\rangle$
- If $I = I'$ and the diagrams differ in the subdiagrams below this common chord, promote the separating functionary of the subdiagrams by plugging simultaneously:
$$d \;\mapsto\; \langle a\, b\, c\, n\rangle\, d - \langle a\, b\, d\, n\rangle\, c\;, \qquad n \;\mapsto\; \langle a\, b\, c\, d\rangle\, n - \langle a\, b\, c\, n\rangle\, d + \langle a\, b\, d\, n\rangle\, c$$
- Otherwise, they differ in some chords to the left of the rightmost top chord, and then promote the separating functionary of these subdiagrams by substituting:
$$b \;\mapsto\; \langle a\, c\, d\, n\rangle\, b - \langle b\, c\, d\, n\rangle\, a$$

Surjectivity

Theorem 5 asserts that the closure of all BCFW images covers the amplituhedron. Our proof relies on a detailed analysis of the codimension-one adjacencies between cells.

First, we characterize each BCFW cell by inequalities on domino matrix terms and on 2-by-2 minors. We also show that every codimension-one boundary of a BCFW positroid cell either maps to a codimension-one stratum in the interior of $\mathcal{A}_{n,k,4}$ or to the topological boundary $\partial\mathcal{A}_{n,k,4}$. We then verify that every such interior boundary is shared by exactly two BCFW cells. These adjacencies can be characterized in combinatorial terms, such as shifting by one a head or a tail of one chord. For a simple example in Figure 2, one can see that $\delta_1 \to 0$ in (B) matches $\gamma_1 \to 0$ in (C). Other adjacency rules are a bit more complicated and carefully described in [16, Section 7]. In $\mathcal{A}_{7,2,4}$ they yield boundaries between: (D)-(E), (E)-(F), (B)-(C), (B)-(D), (B)-(E), (A)-(C), (A)-(E), (A)-(F).

The idea of the surjectivity proof in [16, Section 8] is topological – you cannot escape the image of the BCFW cells. Every path between two points in the interior can be perturbed to a transversal path that avoids codimension-two strata of BCFW images. Then, as you travel along, whenever you exit one BCFW image, there is always another BCFW image from the other side, because every internal codimension-one stratum is shared by two disjoint cells. If there were an interior point outside the closures of all BCFWs, then we could have reached it by path-connectivity and obtain a contradiction.

Acknowledgements

The authors thank Nima Arkani-Hamed, Matteo Parisi, Melissa Sherman-Bennett and Lauren Williams for interesting discussions in relation to this work. R.T. would like to thank Jian-Rong Li, Xavier Blot and Yoel Groman for helpful discussions. The authors thank the IT team in the Computer Science and Mathematics Department of the Weizmann Institute, and especially Unix engineer Amir Gonen, who helped us to run our computations.

References

[1] S. Agarwala and C. Marcott. "Cancellation of spurious poles in N=4 SYM: physical and geometric". 2021. arXiv:2105.00541.

[2] S. Agarwala and E. Marin-Amat. "Wilson loop diagrams and positroids". *Communications in Mathematical Physics* **350**.2 (2017), pp. 569–601.

[3] N. Arkani-Hamed, Y. Bai, S. He, and G. Yan. "Scattering forms and the positive geometry of kinematics, color and the worldsheet". *J. High Energy Physics* **2018**.5 (2018), pp. 1–78.

[4] N. Arkani-Hamed, Y. Bai, and T. Lam. "Positive geometries and canonical forms". *Journal of High Energy Physics* **2017**.11 (2017), pp. 1–124.

[5] N. Arkani-Hamed, J. Bourjaily, F. Cachazo, A. Goncharov, J. Trnka, and A. Postnikov. *Grassmannian Geometry of Scattering Amplitudes*. Cambridge University Press, 2016.

[6] N. Arkani-Hamed, J. L. Bourjaily, F. Cachazo, A. Postnikov, and J. Trnka. "On-shell structures of MHV amplitudes beyond the planar limit". *Journal of High Energy Physics* **2015**.6 (2015), pp. 1–16.

[7] N. Arkani-Hamed, S. He, and T. Lam. "Stringy canonical forms". *Journal of High Energy Physics* **2021**.2 (2021), pp. 1–62.

[8] N. Arkani-Hamed, T.-C. Huang, and Y.-t. Huang. "The EFT-hedron". *Journal of High Energy Physics* **2021**.5 (2021), pp. 1–108.

[9] N. Arkani-Hamed, Y.-t. Huang, and S.-H. Shao. "On the positive geometry of conformal field theory". *Journal of High Energy Physics* **2019**.6 (2019), pp. 1–48.

[10] N. Arkani-Hamed, H. Thomas, and J. Trnka. "Unwinding the amplituhedron in binary". *Journal of High Energy Physics* **2018**.1 (2018), pp. 1–41.

[11] N. Arkani-Hamed and J. Trnka. “The amplituhedron”. *Journal of High Energy Physics* **2014**.10 (2014), pp. 1–33.

[12] H. Bao and X. He. “The m=2 amplituhedron”. 2019. arXiv:1909.06015.

[13] J. Bourjaily and H. Thomas. “What is the Amplituhedron”. *Not. Amer. Math. Soc* **65** (2018), p. 167.

[14] R. Britto, F. Cachazo, and B. Feng. “New recursion relations for tree amplitudes of gluons”. *Nuclear Physics B* **715**.1-2 (2005), pp. 499–522.

[15] R. Britto, F. Cachazo, B. Feng, and E. Witten. “Direct proof of the tree-level scattering amplitude recursion relation in Yang–Mills theory”. *Physical review letters* **94**.18 (2005), p. 181602.

[16] C. Even-Zohar, T. Lakrec, and R. J. Tessler. “The Amplituhedron BCFW Triangulation”. 2021. arXiv:2112.02703.

[17] C. Even-Zohar, T. Lakrec, and R. J. Tessler. “bcfw-amp”. Version 1.0.0. 2022. Link.

[18] S. Fomin and A. Zelevinsky. “Double Bruhat cells and total positivity”. *Journal of the American Mathematical Society* **12**.2 (1999), pp. 335–380.

[19] S. Fomin and A. Zelevinsky. “Cluster algebras I: foundations”. *Journal of the American Mathematical Society* **15**.2 (2002), pp. 497–529.

[20] S. Fomin and A. Zelevinsky. “Cluster algebras II: Finite type classification”. *Inventiones Mathematicae* **154**.1 (2003), p. 63.

[21] P. Galashin, S. Karp, and T. Lam. “Regularity theorem for totally nonnegative flag varieties”. *Journal of the American Mathematical Society* **35**.2 (2022), pp. 513–579.

[22] P. Galashin, S. N. Karp, and T. Lam. “The totally nonnegative Grassmannian is a ball”. *Advances in Mathematics* **397** (2022), p. 108123.

[23] P. Galashin and T. Lam. “Parity duality for the amplituhedron”. *Compositio Mathematica* **156**.11 (2020), pp. 2207–2262.

[24] A. Hodges. “Eliminating spurious poles from gauge-theoretic amplitudes”. *Journal of High Energy Physics* **2013**.5 (2013), pp. 1–23.

[25] S. N. Karp and L. K. Williams. “The m=1 Amplituhedron and Cyclic Hyperplane Arrangements”. *International Mathematics Research Notices* **2019**.5 (2019), pp. 1401–1462.

[26] S. N. Karp, L. K. Williams, and Y. X. Zhang. “Decompositions of amplituhedra”. *Annales de l’Institut Henri Poincaré D* **7**.3 (2020), pp. 303–363.

[27] Y. Kodama and L. Williams. “Combinatorics of KP solitons from the real Grassmannian”. *Algebras, Quivers and Representations*. Springer, 2013, pp. 155–193.

[28] Y. Kodama and L. Williams. “KP solitons and total positivity for the Grassmannian”. *Inventiones mathematicae* **198**.3 (2014), pp. 637–699.

[29] T. Lam. “Totally nonnegative Grassmannian and Grassmann polytopes”. *Current Developments in Mathematics* **2014**.1 (2014), pp. 51–152.

[30] T. Lam. "An invitation to positive geometries". 2022. arXiv:2208.05407.

[31] T. Łukowski and R. Moerman. "Boundaries of the Amplituhedron with amplituhedron-Boundaries". *Computer Physics Communications* **259** (2021), p. 107653.

[32] T. Łukowski, M. Parisi, M. Spradlin, and A. Volovich. "Cluster adjacency for m=2 Yangian invariants". *Journal of High Energy Physics* **2019**.10 (2019), pp. 1–11.

[33] T. Łukowski, M. Parisi, and L. K. Williams. "The positive tropical Grassmannian, the hypersimplex, and the m=2 amplituhedron". 2020. arXiv:2002.06164.

[34] G. Lusztig. "Total positivity in reductive groups". *Lie theory and geometry*. Springer, 1994, pp. 531–568.

[35] R Marsh and K. Rietsch. "Parametrizations of flag varieties". *Representation Theory of the American Mathematical Society* **8**.9 (2004), pp. 212–242.

[36] F. Mohammadi, L. Monin, and M. Parisi. "Triangulations and canonical forms of amplituhedra: a fiber-based approach beyond polytopes". *Communications in Mathematical Physics* **387**.2 (2021), pp. 927–972.

[37] M. Parisi, M. Sherman-Bennett, and L. Williams. "The m=2 amplituhedron and the hypersimplex: signs, clusters, triangulations, Eulerian numbers". 2021. arXiv:2104.08254.

[38] A. Postnikov. "Total positivity, Grassmannians, and networks". 2006. arXiv:math/0609764.

[39] A. Postnikov. "Positive Grassmannian and polyhedral subdivisions". *Proc. of the International Congress of Mathematicians: Rio de Janeiro 2018*. World Scientific. 2018, pp. 3181–3211.

[40] K Rietsch. "Closure relations for totally nonnegative cells in G/P". *Mathematical Research Letters* **13**.5-6 (2006), pp. 775–786.

[41] K. Rietsch. "An algebraic cell decomposition of the nonnegative part of a flag variety". *Journal of algebra* **213**.1 (1999), pp. 144–154.

[42] K. C. Rietsch. "Total positivity and real flag varieties". PhD thesis. Massachusetts Institute of Technology, 1998.

[43] D. Speyer and L. Williams. "The tropical totally positive Grassmannian". *Journal of Algebraic Combinatorics* **22**.2 (2005), pp. 189–210.

[44] D. Speyer and L. Williams. "The positive Dressian equals the positive tropical Grassmannian". *Transactions of the American Mathematical Society, Series B* **8**.11 (2021), pp. 330–353.

[45] B. Sturmfels. "Totally positive matrices and cyclic polytopes". *Linear Algebra and its Applications* **107** (1988), pp. 275–281. DOI.

[46] J. Trnka. "Towards the Gravituhedron: new expressions for NMHV gravity amplitudes". *Journal of High Energy Physics* **2021**.4 (2021), pp. 1–63.

[47] L. Williams and T. Lam. "Total positivity for cominuscule Grassmannians". *Discrete Mathematics & Theoretical Computer Science* (2008).

[48] L. K. Williams. "The positive Grassmannian, the amplituhedron, and cluster algebras". 2021. arXiv:2110.10856.